# Thermal Conductivity of Compacted Sand/Ice Mixtures

RICHARD McGAW, U.S. Army Cold Regions Research and Engineering Laboratory, Hanover, New Hampshire

The thermal conductivities of 20-30 Ottawa sand and 30-100 Ottawa sand, compacted with 30-100 crushed ice, were measured by the probe method of transient heating. A commercially available probe, 0.02 in. in diameter with a length/diameter ratio of 412, was used. Temperatures were 18 and 23 F. Water contents ranged from air-dry to 100 percent by weight. As the percentage of ice was increased, thermal conductivity increased from the value for air-dry sand to the value for bulk ice. For similar mixtures, the conductivity of the finer sand was higher. For mixtures compared at constant porosity, thermal conductivity decreased with the percentage of sand. Since the conductivity of quartz is 3.5 times that of ice, it was concluded that contact resistance at the interface between sand and ice at 18 F must be high. Thermal conductivity at 23 F was higher than at 18 F. It appeared that a reduction in contact resistance with temperature was responsible. Kersten's 1949 data for sandy soils at 25 F compared favorably with the results for the sand/ice mixtures.

•THE thermal conductivity of a soil is one of the major factors influencing the rate at which freezing temperatures penetrate into the ground under natural conditions. Of particular interest is the conductivity in the frozen zone where temperatures are close to 32 F.

Kersten (1) used a steady-state method to measure the thermal conductivities of various soils in the laboratory at temperatures of 25 and 40 F. Kersten's method required a temperature differential of 10 F, corresponding to an average gradient of 5 F/in. and heating periods of many hours. There was evidence of moisture and vapor migration in many of his tests. The laboratory study reported here used a transient heating technique to measure the thermal conductivity of frozen quartz sand at 18 and 23 F (-8 C and -5 C). This method required a differential of only 2 F corresponding to an average gradient of 1 F/in., and heating periods of 10 min or less. Vapor migration was minimal.

The investigation utilized the probe method in which a constant rate of heat production along an axial source produces an expanding cylindrical temperature field in the test material. Previous application of the probe method to frozen soils has been slight. Lachenbruch (2) used a thermal probe at Barrow, Alaska, to measure the in situ conductivities of frozen and thawed soils, snow, and sea ice. Wechsler (3) performed some exploratory laboratory tests on frozen soils under contract to USA CRREL to evaluate several types of probes. These studies indicated that the probe method should be a convenient and suitable tool for measuring the thermal conductivity of frozen soils near the freezing point. The purpose of the tests described here was to investigate the applicability of the method to frozen sands. Further tests are planned using fine-grained soils.

---

Paper sponsored by Committee on Frost Action and presented at the 47th Annual Meeting.

## PROBE THEORY

The probe method of measuring thermal conductivity is based on the line heat-source method, which utilizes a heated wire. Van der Held and Van Drunen (4) first used the line-source method to measure the conductivity of liquids. Line-source theory results in a simple expression for thermal conductivity.

Beginning from an isothermal condition, the temperature rise at a distance r from the line-source, during the heating time t, is given by

$$T = \frac{q}{4\pi K}\left[ \ln \frac{4\alpha t}{r^2} - \gamma - \left(\frac{r^2}{4\alpha t}\right) + \tfrac{1}{4}\left(\frac{r^2}{4\alpha t}\right)^2 + \ldots \right] \tag{1}$$

where q is a constant heating rate per unit length of source, K and $\alpha$ are the thermal conductivity and diffusivity of the test medium, and $\gamma = 0.5772$. With r small and t large enough that $(r^2/4\,\alpha\, t) \ll 1$, Eq. 1 reduces to

$$T = \frac{q}{4\pi K}\left[ \ln t + \left(\ln \frac{4\alpha}{r^2} - \gamma\right) \right] \tag{2}$$

With $\alpha$ and r unchanging, the expression in parentheses is a constant, so that the temperature rise plotted against the logarithm of time will be a straight line. The temperature rise between any two successive large times is

$$\Delta T = \frac{q}{4\pi K} \ln \frac{t_2}{t_1} \tag{3}$$

the value of the conductivity being given by

$$K = \frac{q}{4\pi \Delta T} \ln \frac{t_2}{t_1} \tag{4}$$

Thus after a short initial period of heating, the conductivity of the test material can be calculated from the slope of the graph of temperature rise vs the logarithm of time.

The probe, or portable heating element, was introduced by Hooper and Lepper (5) to measure the thermal conductivity of soils in situ. Investigators using various probes soon found that the dimensions and thermal properties of the probe, and its contact resistance with the test material, all influenced the observed temperature rise. Equations for the temperature rise at the probe contain more terms than the equations just listed; however, with proper design and handling of the probe, the simplicity of the line-source method can be essentially duplicated.

Solutions for the temperature rise at the inner radius of a hollow metal probe, heated along its outer radius b, have been given by Blackwell (6). If the probe has a heat capacity MC per unit of length and a contact resistance 1/H per unit of area, the temperature at the probe after the first seconds of heating is given by

$$T = \frac{q}{4\pi K}\left\{ \ln 4\tau - \gamma + \frac{2K}{bH} + \frac{1}{2\tau} \right.$$
$$\left. \left[ \ln 4\tau - \gamma + 1 - \frac{2}{\beta}\left(\ln 4\tau - \gamma + \frac{2K}{bH}\right) \right] + 0\left(\frac{1}{\tau^2}\right) \right\} \tag{5}$$

where $\tau = \alpha\, t/b^2$ and $\beta = 2\pi\, b^2 mc/MC$; mc is the volumetric heat capacity of the test material.

In a related solution, Blackwell (6) concluded that the finite conductivity of the probe material will produce no significant change in Eq. 5. Nor does it matter whether the probe is considered to be hollow or solid, for Jaeger (7) found an identical solution on the assumption of a solid probe. Eq. 5 may therefore be accepted as the basic equation for the temperature rise at a probe.

Heat losses along the axis of the probe can cause deviations from Eq. 5 of unknown amounts, and should be eliminated to the extent possible. Lentz (8) and Hooper and Chang (9) drew attention to heat conduction through the electrical and thermocouple leads, which can be controlled by applying thermal insulation. Blackwell (10) found that temperature gradients along the probe itself will be negligible if it is of good conducting material and the length is at least 25 times the diameter.

For times sufficiently large that $r^2/4\,\alpha\,t << 1$ ($\tau >> 1/4$), terms proportional to powers of $1/\tau$ can be neglected in Eq. 5. For large times, the temperature rise at the probe is therefore

$$T = \frac{q}{4\pi K}\left(\ln 4\tau - \gamma + \frac{2K}{bH}\right) \tag{6a}$$

or

$$T = \frac{q}{4\pi K}\left[\ln t + \left(\ln \frac{4\alpha}{b^2} - \gamma + \frac{2K}{bH}\right)\right] \tag{6b}$$

Since b and $\gamma$ are absolute constants, the expression in parentheses is a constant when $\alpha$, K, and $1/H$ are unchanging during a test. In this case, the temperature rise between successive large times reduces to the line-source relation (Eq. 3). Eq. 4 then gives the value of thermal conductivity for the probe method as well as for the line heat-source method.

Successful use of the probe method depends to a large extent on maintaining the thermal properties of the test material, the contact resistance with the probe, and the heat input constant during the test interval. Small temperature differentials, attention to the physical contact between the probe and the soil, and control of axial heat losses through proper design will ordinarily insure these conditions to an adequate degree.

## MATERIALS AND METHODS

The soils tested were Ottawa standard sand (20-30 mesh) and graded Ottawa sand (30-100 mesh) at water contents ranging from air-dry to 100 percent by weight. To insure homogeneity, specimens were not frozen in place as were Kersten's. The air-dry sand was mixed with 30-100 mesh crushed ice and compacted in layers at 12 F (-11 C) to the maximum attainable density. Table 1 gives the physical condition of the test specimens after compaction. Figures 1 and 2 show volume and water content relationships in the compacted specimens.

TABLE 1

CONDITION OF COMPACTED SPECIMENS

| Soil Type | Water Content | | Weight | | Total Volume (cc) | Unit Weight | | Volume Fraction | | Volume Total Solids (%) | Porosity (%) | Void Ratio | Volume Ratio: Ice/Solids (%) |
|---|---|---|---|---|---|---|---|---|---|---|---|---|---|
| | Nom. (%) | Actual (%) | Sand (gm) | Ice (gm) | | Sand (gm/cc) | Ice (gm/cc) | Sand (%) | Ice (%) | | | | |
| No. 20-30 Standard Ottawa Sand | 0 | 0.05 | 1728 | 0 | 1015 | 1.70 | 0.00 | 64.2 | 0.0 | 64.2 | 35.8 | 0.558 | 0.0 |
| | 10 | 9.5 | 1432 | 136 | 1000 | 1.43 | 0.14 | 54.0 | 14.8 | 68.8 | 31.2 | 0.454 | 21.5 |
| | 20 | 20.1 | 1206 | 243 | 1000 | 1.21 | 0.24 | 45.5 | 26.3 | 71.8 | 28.2 | 0.393 | 36.6 |
| | 40 | 37.7 | 949 | 358 | 1000 | 0.95 | 0.36 | 35.8 | 39.0 | 74.8 | 25.2 | 0.337 | 52.2 |
| | 60 | 58.6 | 763 | 447 | 1000 | 0.76 | 0.45 | 28.8 | 48.4 | 77.2 | 22.8 | 0.295 | 62.7 |
| | 100 | 95.4 | 543 | 518 | 1000 | 0.54 | 0.52 | 20.5 | 56.1 | 76.6 | 23.4 | 0.306 | 73.2 |
| No. 30-100 Graded Ottawa Sand | 0 | 0.05 | 1785 | 0 | 1000 | 1.79 | 0.00 | 67.4 | 0.0 | 67.4 | 32.6 | 0.484 | 0.0 |
| | 10 | 10.0 | 1468 | 147 | 1000 | 1.47 | 0.15 | 55.4 | 16.0 | 71.4 | 28.6 | 0.400 | 22.4 |
| | 25 | 24.8 | 1149 | 287 | 1000 | 1.15 | 0.29 | 43.4 | 31.3 | 74.7 | 25.3 | 0.339 | 41.9 |
| | 40 | 37.5 | 965 | 362 | 1000 | 0.97 | 0.36 | 36.4 | 39.5 | 75.9 | 24.1 | 0.318 | 52.0 |
| | 40 | 39.8 | 939 | 375 | 1000 | 0.94 | 0.38 | 35.4 | 40.9 | 76.3 | 23.7 | 0.311 | 53.6 |
| | 100 | 96.9 | 543 | 526 | 1000 | 0.54 | 0.53 | 20.5 | 57.4 | 77.9 | 22.1 | 0.284 | 73.7 |
| No. 30-100 Crushed Ice | ∞ | ∞ | 0 | 638 | 1000 | 0 | 0.64 | 0 | 69.6 | 69.6 | 30.4 | 0.437 | 100.0 |

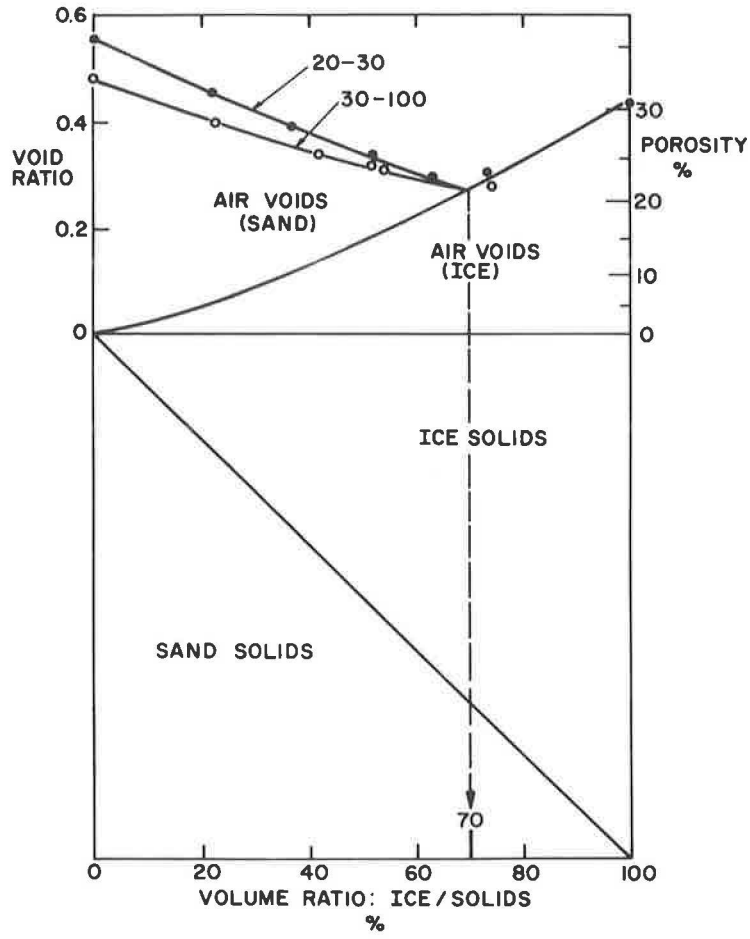


Figure 1. Compaction results (I): packing diagram (12 F).

Compaction was performed in separate containers (Fig. 3), which were cut to length from standard aluminum pipe. The foot of the tamper used was 2.5 in. in diameter and 3.25 in. high, giving a specimen volume of 1000 cc when the tamper was flush with the top of the container. Specimens were stored in the containers at 12 F and brought to the test temperature immediately before testing. Colder tests were performed first so that the test temperature was the warmest a given specimen had undergone.

The probe used in the investigation was Pittsburgh Corning Model CS-48, available commercially from Custom Scientific Instruments. A schematic of the probe construction is shown in Figure 4. A stainless steel sheath of 0.02 in. outside diameter contains a bifilar heating coil of constantan wire (1523 ohms), within which is placed a chromel/constantan thermocouple at mid-length. A molded plastic block supports the thermocouple and power leads. The free length of the probe below the block is 8.24 in., resulting in a length/diameter ratio of 412.

Although sturdily constructed, the probe was too flexible to force into the dense mixtures of sand and ice. A hole 0.04 in. in diameter was therefore drilled along the axis of each specimen to receive the probe. After insertion of the probe, air-dry

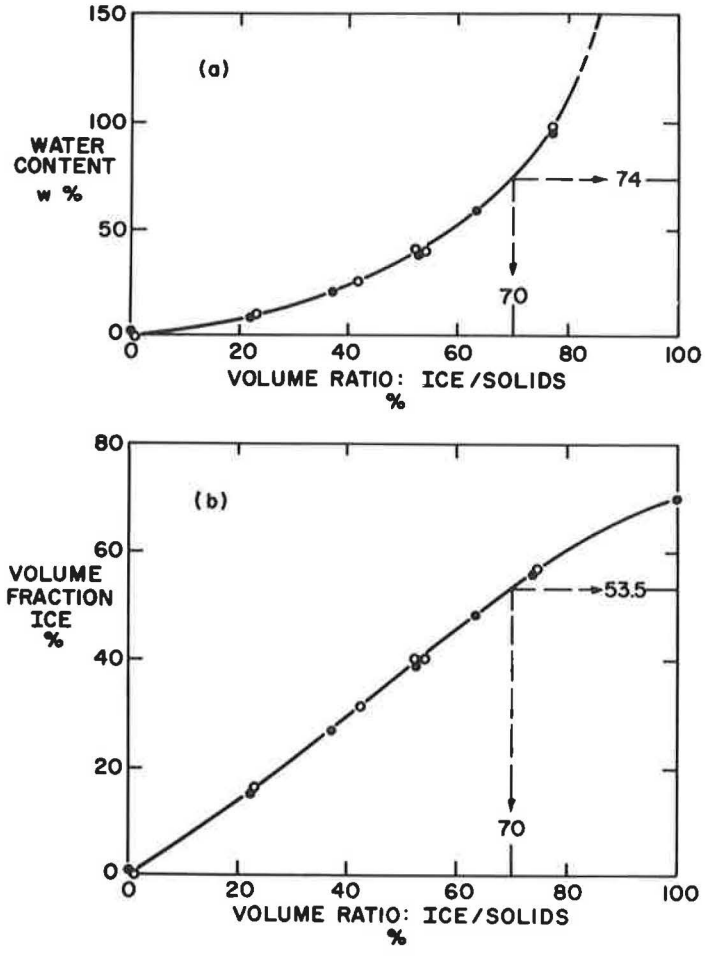


Figure 2. Compaction results (II).

specimens were gently tamped to insure good thermal contact; a small air gap remained around the probe in the others. Because of the porous nature of the specimens, foreign substances were not used in an attempt to improve the contact.

Prior to a test, the specimen container was fitted snugly into an aluminum cooling well (Fig. 5), which was bathed by precooled ethylene glycol. A sealed air chamber provided insulation from the room temperature, which was maintained at 59 F (15 C). Foam insulation was placed around the cooling well assembly and above the specimen container after the probe was in place. The specimen was then allowed to come to equilibrium with the test temperature.

Circuitry consisted of the probe heater circuit, the probe thermocouple circuit, and a monitoring circuit (Fig. 6). The heater circuit contained the probe coil, a switch, a DC milliameter, and a regulated DC voltage power supply. Heat input to the coil was read as $I^2R$, with three predetermined inputs being used, corresponding to 1.5, 3.0, and 6.0 milliwatts per inch of probe.

The probe thermocouple circuit contained the chromel/constantan probe junction, a reference junction in an ice bath, a bias voltage (Medistor Model C-2 microvolt

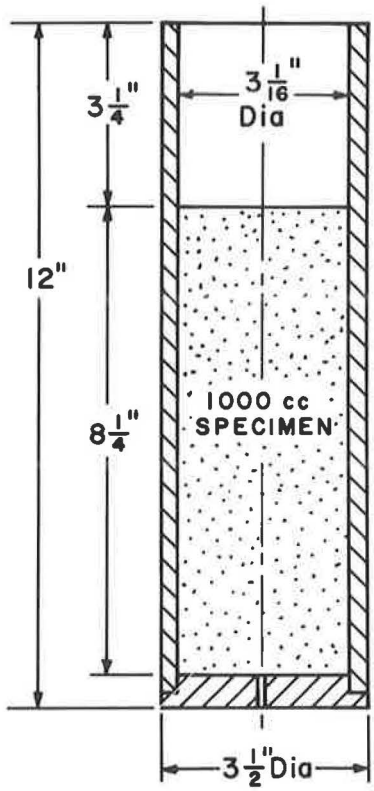


Figure 3. Specimen container.

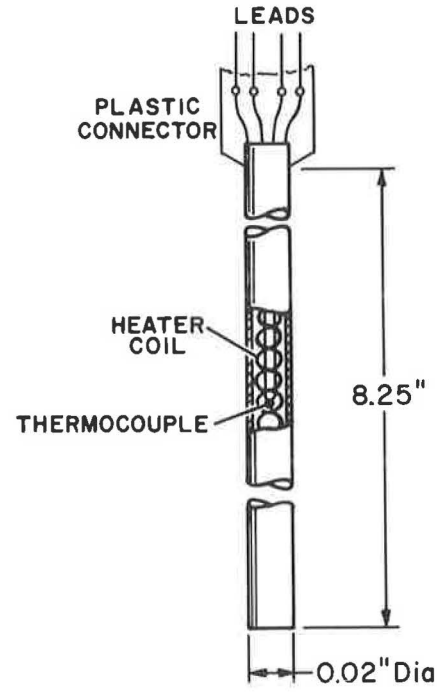


Figure 4. Schematic: Pittsburgh Corning Thermal Conductivity Probe, Model CS-48.

source, accuracy 0.1 percent), an indicating amplifier, and a millivolt recorder. The recorder was operated zero-left with +20 microvolts full scale. After a test had begun, a single bias voltage was selected to maintain the trace on the recorder scale from about 10 sec of heating: linearity of the trace has usually been established by 30 sec of heating. At any time the probe junction temperature could be read as the algebraic sum of the scale voltage (+) and the selected bias voltage (±).

The monitoring circuit contained two copper/constantan thermocouples. One thermocouple, mounted at mid-height in a groove cut into the aluminum cooling well, monitored the temperature of the well and the outside edge of a test specimen. The second thermocouple was inserted next to the probe at the top of a soil specimen, and it was used to check on temperature gradients along the probe. The reference junction was put into the ice bath used for the probe circuit.

The temperature of the ethylene glycol coolant was regulated in a bath through which refrigerant from the laboratory supply lines was constantly circulated. A Bayley precision controller actuated a heater immersed in the glycol, while a 1500 rpm fan continuously circulated the glycol through the bath and the cooling well assembly. Regulation was such that the inner wall of the cooling well ordinarily varied by no more than several microvolts (0.1 F) over a period of weeks.

A typical heating curve is shown in Figure 7, the points having been plotted from the recorder trace. A straight line drawn through the points has a slope ($\Delta T_1$) equal to

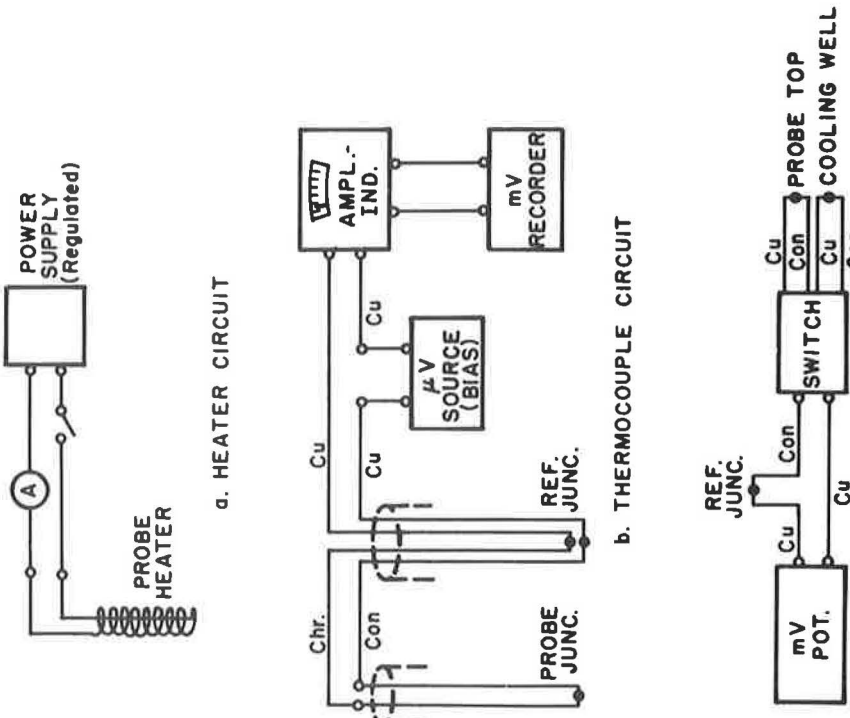


Figure 6. Schematic circuits.

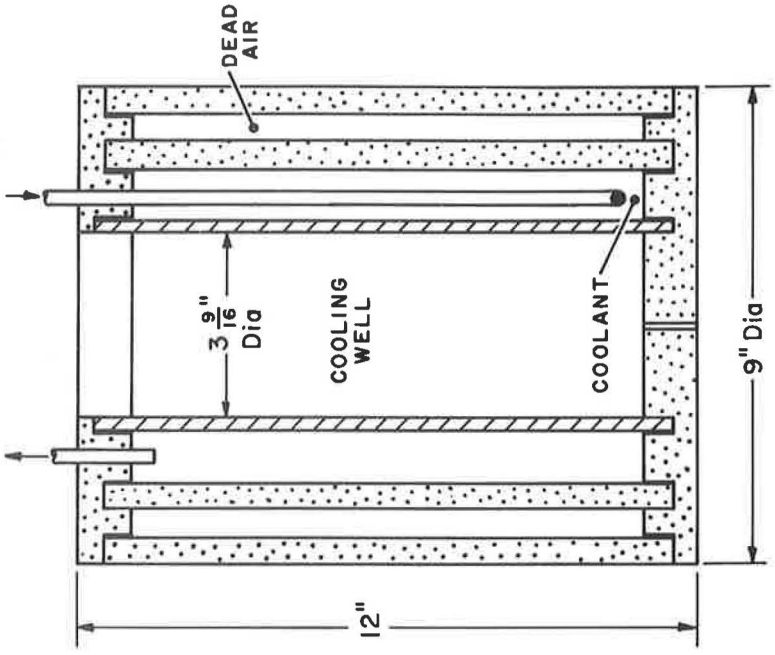


Figure 5. Cooling well assembly.

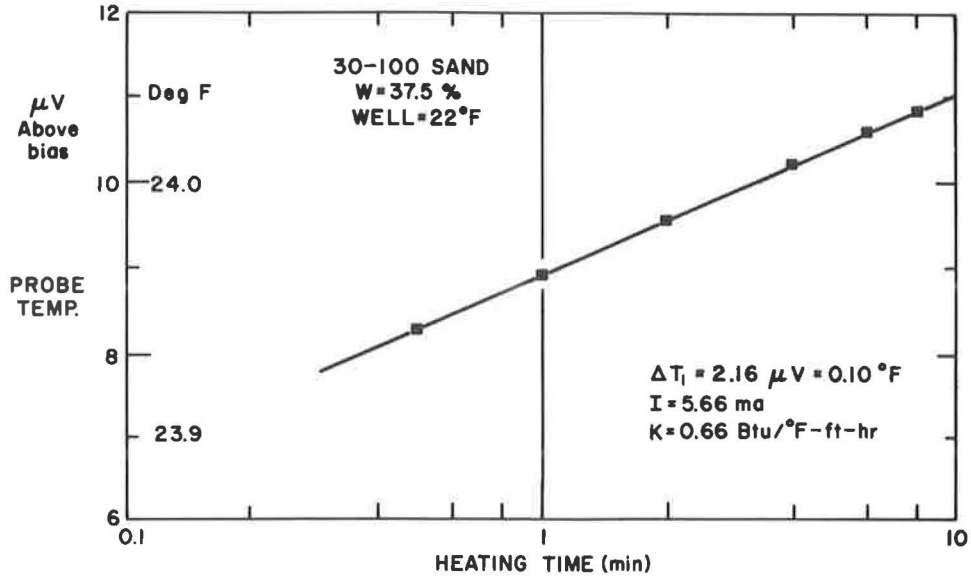


Figure 7. Typical heating curve: 30-100 Ottawa sand (w = 37.5 percent).

2.16 $\mu$V over a single $\log_{10}$ cycle of time. Thermal conductivity in Btu/deg F-ft-hr is calculated from the expression

$$K = \frac{44.6}{\Delta T_1} I^2 \times 10^{-3}$$

which was derived from the probe resistance and Eq. 4. The value of I is measured directly in milliamps for each test.

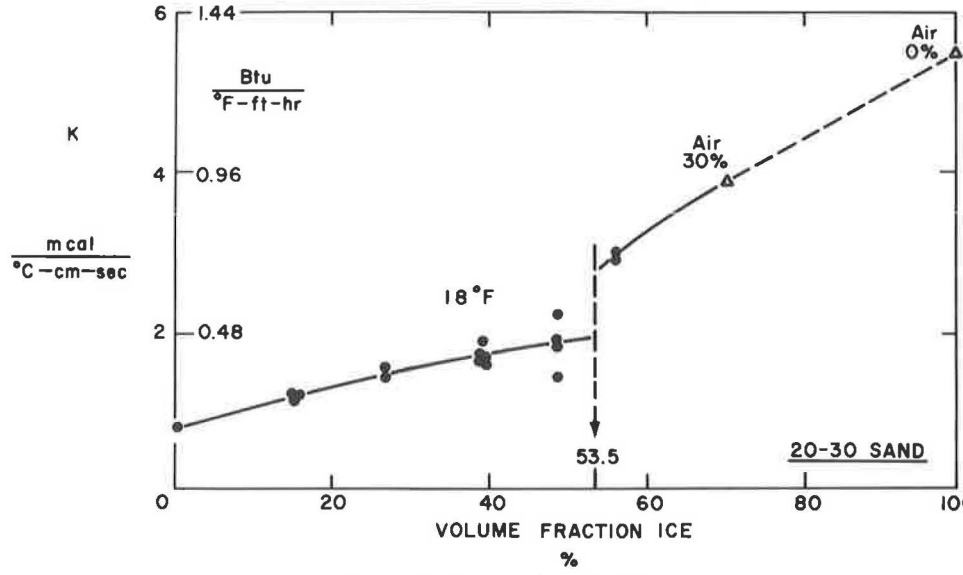


Figure 8. Test results: 20-30 Ottawa sand.

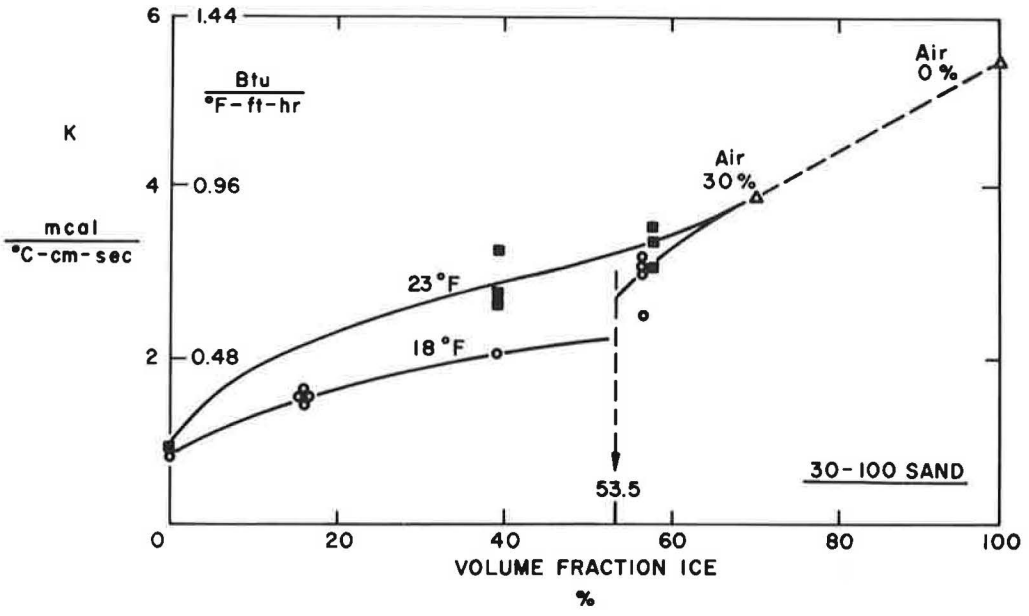


Figure 9. Test results: 30-100 Ottawa sand.

TABLE 2

TEST DATA

| Soil Type | Water Content | | Power Input (mw/in) | Wall Temp. (deg F) | Probe Temp. | | Avg. Temp. (deg F) | Period of Linearity (min) | Type of Test | Conductivity (Btu/deg F-ft-hr) |
|---|---|---|---|---|---|---|---|---|---|---|
| | Nom. (%) | Actual (%) | | | Initial (deg F) | Max. (deg F) | | | | |
| No. 20-30 | 0 | 0.05 | 6.0 | 16.5 | 17.2 | 18.7 | 17.6 | 0.5-6 | heating | 0.187 |
| Standard | 10 | 9.5 | 6.0 | 16.5 | 17.2 | 18.7 | 17.6 | 1.0-9 | heating | 0.286 |
| Ottawa | | | 6.0 | 16.5 | 17.1 | 18.5 | 17.6 | 1.0-10 | heating | 0.283 |
| Sand | | | 6.0 | 16.5 | 17.1 | 18.5 | 17.6 | 1.0-10 | heating | 0.269 |
| | 20 | 20.1 | 6.0 | 16.5 | 17.1 | 18.9 | 17.6 | 0.5-6 | heating | 0.365 |
| | | | 6.0 | 16.5 | 17.1 | 19.8 | 18.1 | 1.0-8 | heating | 0.331 |
| | 40 | 37.7 | 6.0 | 16.5 | 17.1 | 20.1 | 18.3 | 0.5-6 | heating | 0.384 |
| | | | 3.0 | 16.5 | 17.1 | 18.7 | 17.6 | 0.5-10 | heating | 0.377 |
| | | | 3.0 | 16.5 | 17.2 | 18.0 | 17.2 | 0.3-5 | heating | 0.449 |
| | | | 6.0 | 16.5 | 17.2 | 18.7 | 17.6 | 1.0-10 | heating | 0.403 |
| | | | 6.0 | 16.5 | – | 17.4 | 17.1 | 0.5-2 | cooling | 0.413 |
| | 60 | 58.6 | 3.0 | 16.5 | 17.1 | 18.3 | 17.4 | 0.5-10 | heating | 0.425 |
| | | | 3.0 | 16.5 | 17.1 | 18.5 | 17.4 | 0.5-6 | heating | 0.341 |
| | | | 6.0 | 16.5 | 17.4 | 19.8 | 18.1 | 0.5-10 | heating | 0.446 |
| | | | 6.0 | 16.5 | 17.2 | 18.9 | 17.6 | 0.5-6 | heating | 0.528 |
| | 100 | 95.4 | 6.0 | 16.5 | 17.1 | 18.9 | 17.8 | 0.2-1.0 | heating | 0.691 |
| | | | 6.0 | 16.5 | – | 17.2 | 16.9 | 0.5-5 | cooling | 0.718 |
| No. 30-100 | 0 | 0.05 | 6.0 | 16.5 | 17.2 | 18.7 | 17.6 | 0.5-6 | heating | 0.187 |
| Graded | 10 | 10.0 | 3.0 | 16.5 | 17.2 | 18.3 | 17.4 | 0.5-10 | heating | 0.329 |
| Ottawa | | | 3.0 | 16.5 | 17.2 | 18.3 | 17.4 | 0.5-10 | heating | 0.358 |
| Sand | | | 3.0 | 16.5 | 17.2 | 18.3 | 17.4 | 0.5-10 | heating | 0.358 |
| | | | 3.0 | 16.5 | 17.2 | 18.3 | 17.4 | 0.3-9 | heating | 0.377 |
| | 40 | 37.5 | 6.0 | 16.5 | 17.2 | 18.9 | 17.6 | 0.5-8 | heating | 0.475 |
| | 100 | 96.9 | 6.0 | 16.5 | 17.2 | 19.9 | 19.0 | 1.0-10 | heating | 0.715 |
| | | | 6.0 | 16.5 | 17.2 | 19.8 | 19.0 | 1.0-10 | heating | 0.590 |
| | | | 3.0 | 16.5 | 17.4 | 19.6 | 18.0 | 2.0-9 | heating | 0.754 |
| | | | 3.0 | 16.5 | 17.4 | 19.6 | 18.0 | 2.0-9 | heating | 0.722 |
| | 0 | 0.05 | 6.0 | 22.5 | 23.0 | 24.3 | 23.4 | 1.0-10 | heating | 0.200 |
| | 40 | 37.5 | 6.0 | 21.9 | 22.5 | 24.1 | 23.0 | 0.5-8 | heating | 0.660 |
| | | | 6.0 | 21.9 | 22.5 | 24.1 | 23.0 | 0.5-8 | heating | 0.771 |
| | | | 6.0 | 21.9 | 22.5 | 24.1 | 23.0 | 0.5-6 | heating | 0.644 |
| | 100 | 96.9 | 6.0 | 21.9 | – | 22.6 | 22.3 | 2.0-6 | cooling | 0.725 |
| | | | 6.0 | 21.9 | – | 22.6 | 22.3 | 2.0-6 | cooling | 0.807 |
| | | | 6.0 | 21.9 | – | 22.6 | 22.3 | 2.0-7 | cooling | 0.845 |

## RESULTS

Test results for the two sands are shown in Figures 8 and 9. Corresponding data on heat input, temperature, duration of test, etc., are given in Table 2. The abscissa of the graphs is the volume of ice taken as a fraction of total volume. Since the limit of compaction of the crushed ice at 12 F corresponded to a porosity of 30.4 percent (Fig. 1), the dashed portion of the curve from 70 to 100 percent ice is calculated. The basis of the calculation is as follows.

During the preparation of the specimens, the freshly ground ice was observed to sinter rapidly once it has been tightly packed. If left overnight, the ice required shredding through the No. 30 sieve before particles of the original size were recovered. It was therefore concluded that ice grains which are physically in contact after compaction will be bonded. Physical contact between ice grains begins to control the packing arrangement when the ice volume reaches 70 percent of the volume of solids (Fig. 1). Figure 2 indicates that the water content at this point is 74 percent, while the volume fraction of ice is 53.5 percent. Consequently, a virtually continuous matrix of ice may be presumed to exist when the volume of ice exceeds 53.5 percent of the total volume of a specimen.

Because of the practical limits of compaction, when the volume fraction of ice exceeds 70 percent there is no longer sand in the mixture, only ice and air. The thermal conductivity of such an ice/air mixture will be given to a close approximation by the following expression for parallel paths:

$$K = \lambda_i K_i + (1 - \lambda_i) K_a \qquad (7)$$

where $\lambda_i$ is the volume fraction of ice; $K_i$ and $K_a$ are the thermal conductivities of ice and air. At 18 F, the conductivity of ice is given by Dorsey (11) as 5.50 mcal/deg C-cm-sec, or 1.32 Btu/deg F-ft-hr; the conductivity of saturated air at 18 F is given by

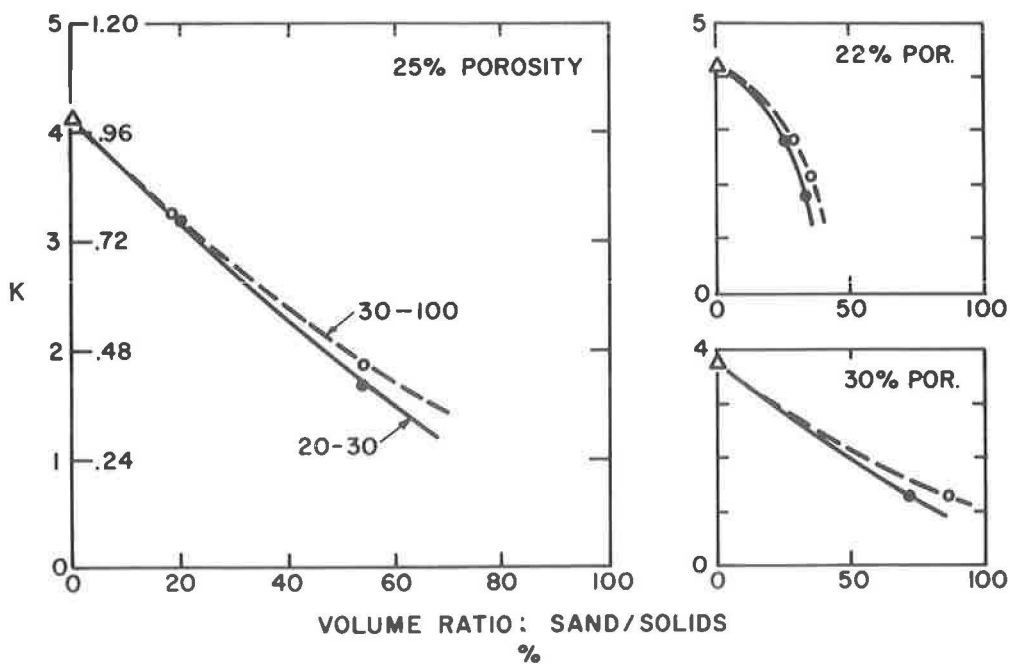


Figure 10. Conductivity vs sand content at constant porosity (18 F).

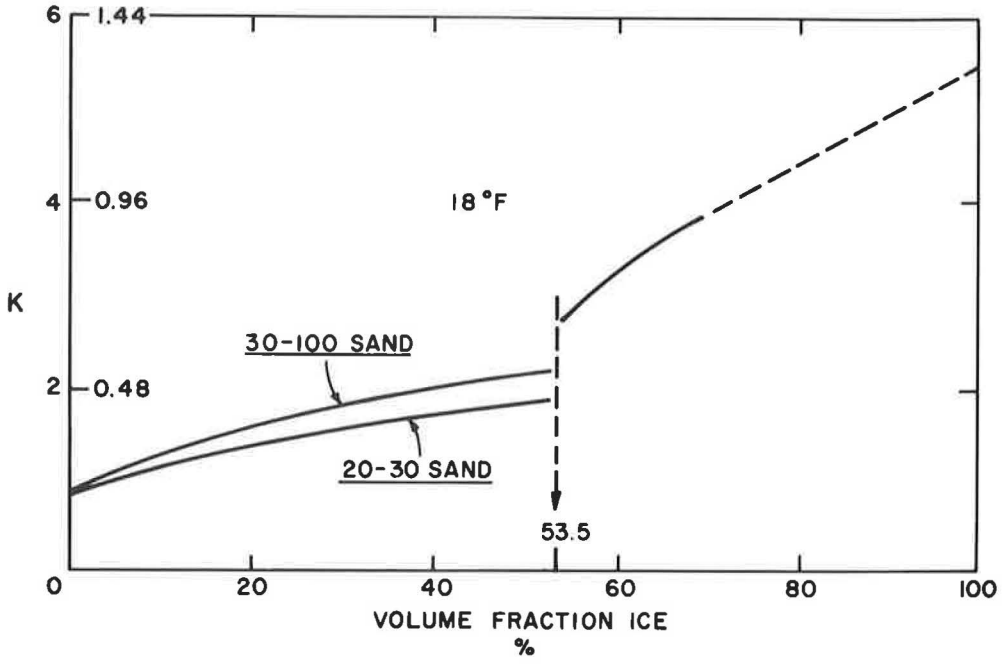


Figure 11. Summary: influence of particle size (18 F).

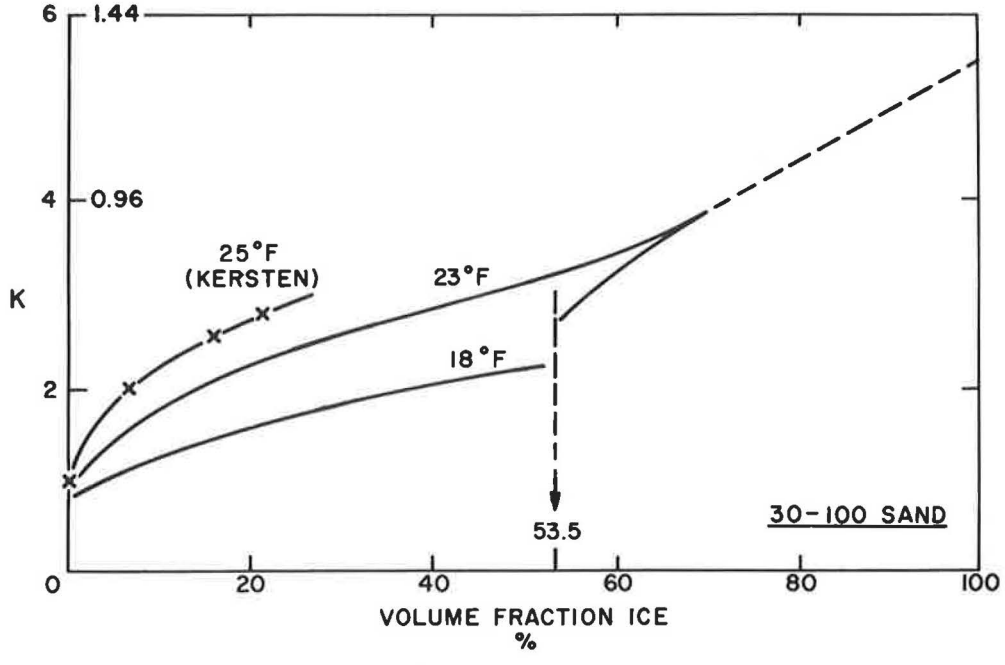


Figure 12. Summary: influence of temperature.

deVries (12) as 0.08 mcal/deg C-cm-sec, or 0.02 Btu/deg F-ft-hr. Values calculated from Eq. 7 are shown in Figures 8 and 9 by triangles. It is evident that the dashed curve is a continuation of the experimental relationship.

A discontinuity in the curves for 18 F marks the point where the ice matrix begins, dividing the curves into distinct branches. One branch corresponds to an ice matrix with imbedded sand, the other to a sand matrix with imbedded ice. Although the average solid conductivity of quartz (4.8 Btu/deg F-ft-hr) is 3.5 times that of ice, the sand matrix branch shows consistently lower conductivities, reaching ultimately the value for air-dry sand at 0 percent ice. Paradoxically, the addition of sand, i.e., a constituent having a higher conductivity than either ice or air, apparently decreases the overall conductance.

Figure 10 shows this result clearly. Here, conductivities taken from Figures 8 and 9 are compared at constant porosity so that only the relative volumes of sand and ice are changing. As the percentage of sand increases, the conductivity of the mixture progressively decreases, the effect being more pronounced at lower porosities. The most likely explanation is that the boundary between sand and ice at 18 F has a high contact resistance, so high in fact that less heat passes through the sand than through the ice it replaced.

The increase of conductivity from 18 to 23 F for the 30-100 sand (Fig. 9) is consistent with this explanation. The increase is certainly not attributable to the conductivities of quartz and ice, for both decrease slightly with temperature. Evidently the primary effect of the temperature increase is a reduction in the contact resistance at the sand-ice boundary.

Figure 11 summarizes the data at 18 F, showing the influence of particle size on thermal conductivity. At a single temperature both gradations gave the same ice-matrix branch, as might be expected when the proportion of sand is low. On the other hand the finer sand developed noticeably higher conductivities in the sand-matrix range. At first thought it would seem that the lower porosities of the 30-100 sand in this range (Fig. 1) would be responsible. However, a comparison at constant porosity (Fig. 10) does not eliminate the differential; for similar mixtures, the finer sand does, indeed, conduct heat more efficiently. Reducing the particle size apparently reduces the contact resistance with ice.

Figure 12 summarizes the data for the 30-100 Ottawa sand and compares them with values found by Kersten (1) for sandy soils at 25 F. Although limited in extent, Kersten's data show the same trend as the data reported here; this will not necessarily be the case for fine-grained soils in which moisture migration could cause differing results. Figure 12 shows the general form of the conductivity relationship to be expected with frozen sandy soils; the discontinuity at the onset of the ice-matrix range should be virtually absent at temperatures of 23 F and warmer.

## CONCLUSIONS

The thermal conductivities of mixtures of sand and ice were measured at 18 and 23 F (-8 C and -5 C), using a transient heating method and a commercially available probe 0.02 in. in diameter. The probe method proved to be highly satisfactory for frozen sands at water contents from 0 percent to 100 percent by weight. The following conclusions may be drawn:

At 18 F, the thermal conductivities of 20-30 Ottawa sand and 30-100 Ottawa sand, compacted with 30-100 crushed ice, had two distinct branches corresponding to a matrix of sand and a matrix of ice. As the percentage of ice was increased, conductivity increased from the value for air-dry sand to the value for bulk ice. There was an abrupt discontinuity at the beginning of the ice matrix range, which was not present at 23 F.

At 18 F, an increase in percentage of sand at constant porosity resulted in a decrease in thermal conductivity. It was concluded that high contact resistance between sand and ice at this temperature is responsible for the decrease.

At 18 F, the conductivity of the finer sand was approximately 20 percent higher in the sand-matrix range than the conductivity of the coarser sand; the ice-matrix range

was identical. It appears that the contact resistance of sand with ice is smaller for finer gradations.

At 23 F, the thermal conductivity of 30-100 Ottawa sand was higher than at 18 F. The greatest increase occurred in the sand-matrix range. The major effect of a temperature increase appears to be a reduction in contact resistance at the interfacial boundaries.

Kersten's thermal conductivity data for sandy soils at 25 F compare favorably with the experimental results reported here.

## ACKNOWLEDGMENTS

The suggestions and continuing interest of Pieter Hoekstra of USA CRREL during the course of the investigation are acknowledged with pleasure. The careful work of Specialist John Steele, who helped prepare the specimens, is also sincerely appreciated.

## REFERENCES

1. Kersten, M. S. Laboratory Research for the Determination of the Thermal Properties of Soils. U.S. Engineer Division, St. Paul, Minn., 1949.
2. Lachenbruch, A. H. A Probe for the Measurement of the Thermal Conductivity of Frozen Soils in Place. Trans. Am. Geophys. Union, Vol. 38, No. 5, pp. 691-697, 1957.
3. Wechsler, A. E. Development of Thermal Conductivity Probes for Soils and Insulations. Arthur D. Little, Inc., Cambridge, Mass., 1965.
4. Van der Held, E. F. M., and Van Drunen, F. G. A Method of Measuring the Thermal Conductivity of Liquids. Physica, Vol. 15, No. 10, pp. 865-81, 1949.
5. Hooper, F. C., and Lepper, F. R. Transient Heat Flow Apparatus for the Determination of Thermal Conductivities. Heating, Piping, and Air Conditioning, Vol. 22, No. 8, pp. 129-134, 1950.
6. Blackwell, J. H. A Transient-Flow Method for Determination of Thermal Constants of Insulating Materials in Bulk: Part I, Theory. Jour. Applied Physics, Vol. 25, No. 2, pp. 137-144, 1954.
7. Jaeger, J. C. Conduction of Heat in an Infinite Region Bounded Internally by a Circular Cylinder of a Perfect Conductor. Australian Jour. of Physics, Vol. 9, pp. 167-179, 1956.
8. Lentz, C. P. A Transient Heat Flow Method of Determining Thermal Conductivity. Canadian Jour. of Tech., Vol. 30, pp. 153-166, 1952.
9. Hooper, F. C., and Chang, S. C. Development of the Thermal Conducticity Probe. Trans. Am. Soc. of Heating and Ventilating Engrs., Vol. 59, pp. 463-472, 1953.
10. Blackwell, J. H. The Axial-Flow Error in the Thermal-Conductivity Probe. Canadian Jour. of Physics, Vol. 34, pp. 412-417, 1956.
11. Dorsey, N. E. Properties of Ordinary Water Substance. Reinhold Publ. Corp., New York, 1940.
12. deVries, D. A. Thermal Properties of Soils. In Physics of Plant Environment (W. R. Van Wijk, Editor), Chap. 7, North-Holland Publ. Co., Amsterdam, 1963.